3-D Computational Modeling of Wet Electrostatic Precipitators to Control Submicron Particulate Emissions

Niloofar Farnoosh
Member, IEEE
University of Western Ontario
1151 Richmond St.
London, ON, N6A 3K7, Canada
nfarnoos@uwo.ca

Robert Allan
P. Eng.
TurboSonic Technologies, Inc.
550 Parkside Dr.
Waterloo, N2L 5V4, Canada
rallan@turbosonic.com

Kazimierz Adamiak
Fellow, IEEE
University of Western Ontario
1151 Richmond St.
London, ON, N6A 3K7, Canada
kadamiak@eng.uwo.ca

***Abstract* – In an effort to better understand Wet Electrostatic Precipitator (WESP) performance, three dimensional computational models of single-stage 305mm and 356mm TurboSonic WESPs were developed. The WESP consists of a 5.5m hexagonal tube with a single corona discharge electrode located at the centre of the tube, on which are placed equally spaced disks of saw tooth or smooth design.**

A hybrid Finite Element Method (FEM) and Flux Corrected Transport (FCT) technique was developed to solve the governing equations to obtain the electric field and ionic charge density distribution inside the precipitator. The gas flow distribution, particle charging and motion under electrostatic and aerodynamic forces were obtained by programming some user defined functions (UDF) in FLUENT software. Particles were assumed to be charged by field charging (ionic bombardment) and diffusion charging. The mutual coupling between electrostatic field, fluid dynamics and particulate dynamics were taken into account for the full analysis.

***Index Terms* – Wet Electrostatic Precipitator (WESP), submicron particle collection, particle charging and transport, numerical simulation.**

I. Introduction

In recent years, special environmental concern has been directed towards controlling the emission of ultrafine particles from industrial exhaust gases. These particles penetrate lung tissues more rapidly and have greater toxicity than larger particles. Control technologies such as wet scrubbers, cyclones, bag filters, and electrostatic precipitators (ESPs) are among the conventional methods utilized to reduce particulate emissions. ESPs are widely applied in large power plants, cement plants, incinerators and various boiler applications to remove the dust and fly ash from the exhaust gases, and when fumes and acid mist must also be collected, a wet ESP (WESP) is used to clean the saturated gas stream [1], [2]. Higher collection efficiency, lower pressure drop, lower energy consumption and capability to operate over a wide range of gas temperatures are features of this control technology. In some applications, the WESP is designated as the best available control technology (BACT) by the EPA.

In this device, particles are exposed to the ion flux in the electrostatic field and are simultaneously charged by two mechanisms: field charging (ionic bombardment) and diffusion charging. Particles then move towards the collection tubes under the Coulomb force and are eventually deposited on them and removed by a liquid film. Even though most of the basic phenomena related to particle collection in a WESP are understood, extensive research is still underway on many detailed aspects, such as electrostatic fields, fluid dynamics, charging mechanisms and particle dynamics [3]-[6].

TABLE I
NUMBER OF NODES AND ELEMENTS FOR 305MM AND 356MM TUBES WITH SMOOTH AND SAW TOOTH DISKS

Disk Design	Tube Diameter (mm)	Number of Tetrahedral Elements	Number of Nodes
Smooth	305	272,484	56,598
	356	276,206	57,580
Saw Tooth	305	514,652	107,285
	356	427,813	89,635

II. Computational Model and Procedure

The 3-D computational model of a 5.5m tube of a vertical flow TurboSonic WESP is shown in Fig. 1. Equally spaced disks are mounted at different angles along the discharge electrode in smooth or saw tooth design. The computational domain was discretized with very fine mesh close to the discharge electrode and coarse mesh close to the collecting walls of the hexagonal tube. The total number of nodes and tetrahedral elements are summarized in Table I.

The discharge electrode is energized with a very high negative voltage, generating an ionic space charge density in the WESP tube. The ion charge density and the electric potential distribution inside the WESP model are obtained from the numerical solution of the Poisson and current continuity equations using the FEM-FCT hybrid method [7]. The ambient gas is considered an incompressible Newtonian fluid; thus having constant density and viscosity. Also, the flow is steady and turbulent assuming the k-ε model in FLUENT software. The assumed operating temperature is 78^{o}C at standard atmospheric pressure (101.325 kPa). At this operating condition, the ion mobility is 3.16e-4 $m^2/V{\cdot}s$, airflow viscosity is 2.11e-5 [kg/m·s] and airflow density is 1 kg/m^3. Particles in the gas stream entering the WESP are assumed to be spherical and electrically neutral, moving with a uniform initial velocity equal to the gas velocity. Particles are in the range of 1 nm to 6 μm. The assumed inlet loading to the WESP is 30 mg/m^3 and the particle density is 1200 kg/m^3. The mass flow rate percentage of each particle size

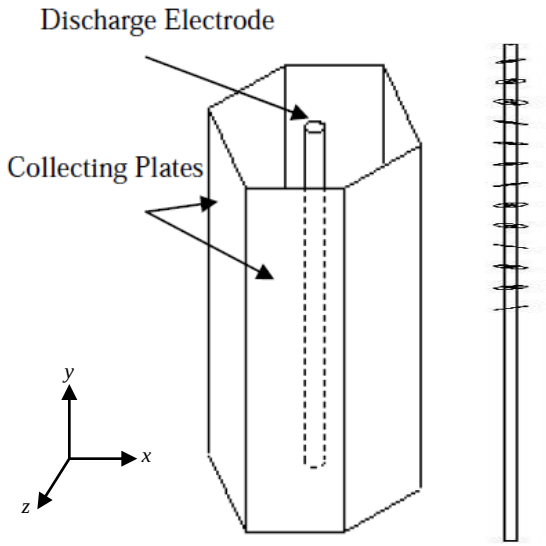

Fig.1. 5.5m Hexagonal Tube with Equally Spaced Disks along the Discharge Electrode.

fraction at the inlet is shown in Fig. 2. The detailed computational procedure can be found in [8]. Due to high computational time and large memory requirements, the major part of these simulations were carried out using SHARCNET super computing network.

III. Results and Discussion

Fig. 3 shows the air flow velocity vectors at $z = 0$ plane in the vicinity of the discharge electrode with saw tooth design for an inlet gas velocity of 2 m/s. Two small vortices can be observed behind each disk. Fig. 4 shows the ionic charge density contours in the same plane when -52 kV is applied to the discharge electrode. The corona discharge is initiated from the tip of spikes on each disk where the electric field intensity is the strongest and the ionic charge density decreases by approaching to the collecting walls of the hexagonal tube.

A. Hexagonal Tube WESP with Smooth Disks

As particles traverse the WESP tube, their charge-to-mass ratio increases up to a saturation level. It was shown that by increasing the inlet gas velocity, the theoretical migration velocity (that component of particle velocity perpendicular to the collecting walls) decreases resulting in collection efficiency reduction [9]. The saturation charge of all particle sizes in terms of number of electrons and the corresponding theoretical migration velocity for inlet gas velocity of 2.7 m/s for a 305mm tube with smooth disks are shown in Fig. 5 and Fig. 6 respectively. It is shown that the theoretical migration velocity versus particle diameter has a minimum between 200 and 300 nm resulting in a minimum in fractional collection efficiency (Grade efficiency) in the same range (Fig. 7). This can be theoretically explained by the two different particle charging methods in the tube; particles smaller than 200 nm are charged by diffusion charging but for particles larger than 300 nm, field charging is more dominant. However, it was

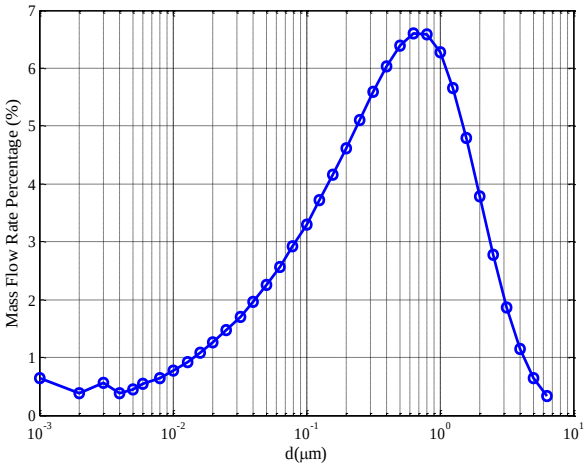

Fig. 2. Mass Flow Rate Percentage of Each Particle Size Fraction at Inlet.

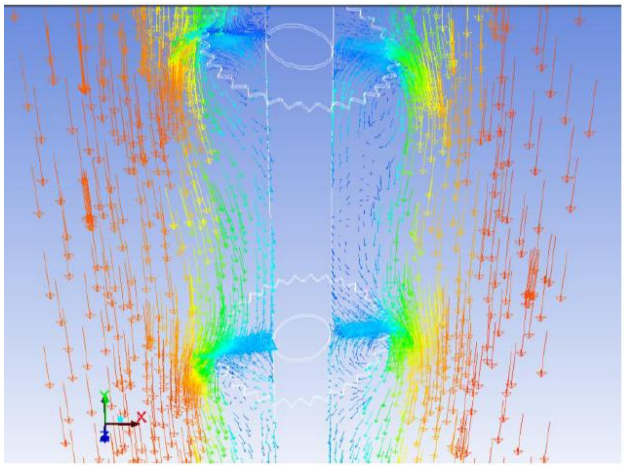

Fig. 3. Velocity Vectors in $z = 0$ Plane, Inlet Gas Velocity is 2 m/s, the Highest Velocity is 2.6 m/s (Red Arrows).

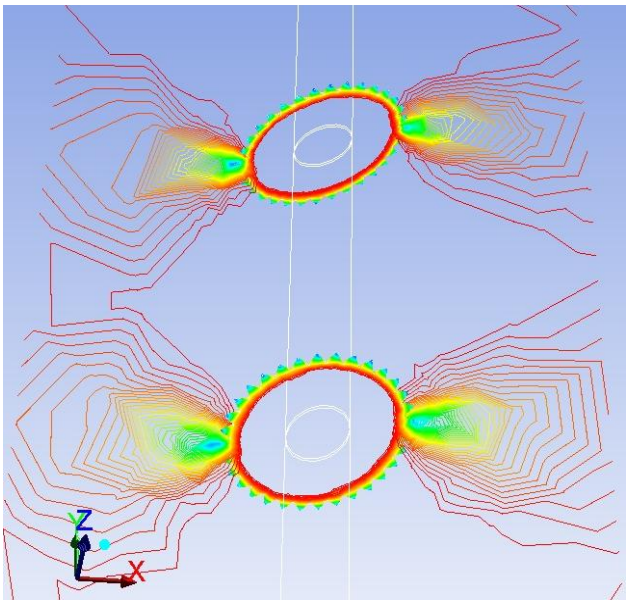

Fig. 4. Ionic Charge Density Contours in $z = 0$ Plane, the Highest Amount of Charge is 142 μC/m^3 Located on Spikes Tips; Number of Contours is 50; Applied Voltage is -52 kV.

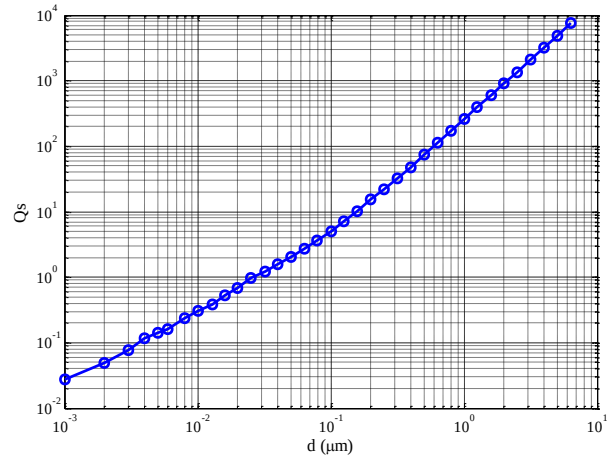

Fig. 5. Saturation Charge versus Particle Diameter in Terms of Number of Electrons for a 305mm Tube with Smooth Disks; Inlet Gas Velocity is 2.7 m/s and Applied Voltage is -80 kV.

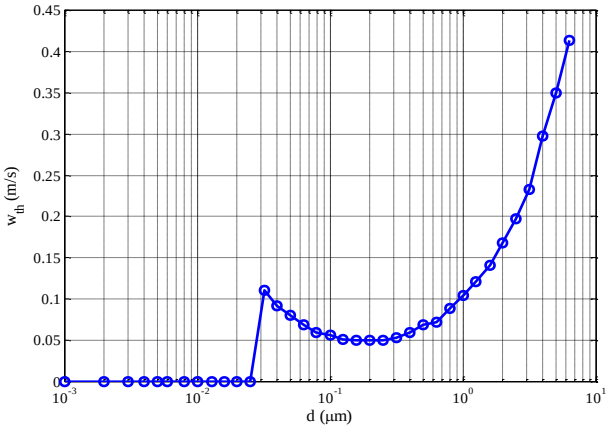

Fig. 6. Theoretical Migration Velocity versus Particle Diameter for a 305mm Tube with Smooth Disks; Inlet Gas Velocity is 2.7 m/s and Applied Voltage is -80 kV.

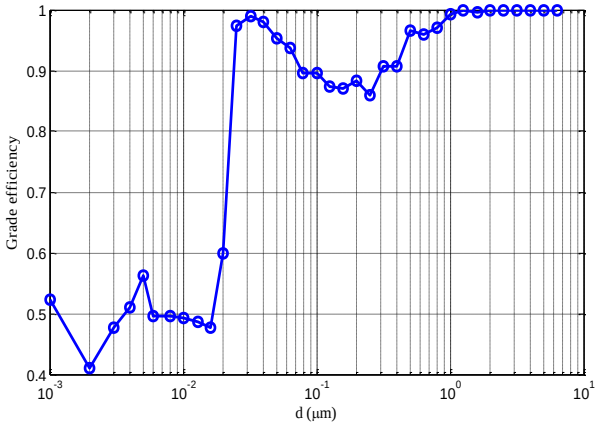

Fig. 7. Fractional Collection Efficiency versus Particle Diameter for a 305mm Tube with Smooth Disks; Inlet Gas Velocity is 2.7 m/s and Applied Voltage is -80 kV.

shown that for inlet gas velocities in the range of 1.2 to 1.8 m/s, the collection efficiency for all particle sizes is above 95%. It is clear that for particles smaller than 30nm, the calculated saturation charge is smaller than 1 electron charge.

TABLE II
TOTAL MASS COLLECTION EFFICIENCY OF A 305MM TUBE WITH SMOOTH DISKS AT DIFFERENT INLET GAS VELOCITIES WITH THE CORRESPONDING EFFECTIVE MIGRATION VELOCITY

Inlet Velocity (m/s)	1.2	1.6	2.0	2.7	3.7	5.5
305mm Tube Operating Point of (-80 kV, 3 mA)	97.6%	96.6%	94.8%	91.1%	83.9%	73.3%
EMV (cm/s)	6.22	7.52	8.21	9.07	9.39	10.9

TABLE III
TOTAL MASS COLLECTION EFFICIENCY OF 305MM AND 356MM TUBES WITH SAW TOOTH DISKS AT DIFFERENT INLET GAS VELOCITIES

Inlet Velocity (m/s)	1.2	1.6	2.0	2.7	3.7	5.5
305mm Tube Operating Point of (-52 kV, 3 mA)	93.4%	90.0%	85.0%	76.9%	67.4%	56.7%
356mm Tube Operating Point of (-61 kV, 3 mA)	91.5%	86.8%	81.2%	71.1%	63.1%	53.9%

Practically, these particles obtain no charge or at least 1 electron charge and are subjected to drag and turbulence dispersion forces rather than electrostatic forces; thus, they cannot be collected by precipitators.

The total mass collection efficiencies and effective migration velocity (EMV) [10] for a 305mm tube with smooth disks at different inlet gas velocities are summarized in Table II. The EMV was calculated with the Deutsch equation. An electrical operating point was chosen from a V-I characteristic curve measured on a full-scale WESP installation. The particle loading effect on corona discharge current was neglected in this part of the simulations and the same operating points were assumed for different gas flow rates.

B. Hexagonal Tube WESP with Saw Tooth Disks

In this section, the simulations were repeated for both 305mm and 356mm tubes with saw tooth electrode design. Fig. 8 shows the fractional collection efficiency of all particle sizes. The total mass collection efficiencies at different inlet gas velocities are summarized in Table III. Different voltages were assumed for each tube diameter; however, the same total discharge current of 3.0 mA was used, which explains the lower efficiency for 356mm tube.

C. Variation of Precipitation Performance with Velocity and Power Input for 305mm Tube with Smooth Disks

Experimental observations from TurboSonic's pilot scale WESP had shown that the EMV is almost constant when the inlet gas velocity increases and then starts to decrease at a specific inlet gas velocity [11]. In Table II, the EMV has been calculated for constant voltage and discharge current of -80 kV and 3 mA over the entire velocity range (Case A).

In practical conditions, the operating voltage cannot be maintained constant at -80 kV. In this case for higher velocities, the total mass collection efficiency and the corresponding EMV for different inlet gas velocities were calculated at discrete operating points chosen from an existing V-I characteristic curve by taking into account the corona discharge current quenching. These data have been presented in Table IV (Case B). The variation of EMV versus inlet gas

TABLE IV
TOTAL MASS COLLECTION EFFICIENCY OF 305MM TUBE WITH SMOOTH DISKS AT DIFFERENT INLET GAS VELOCITIES AND APPLIED VOLTAGES WITH THE CORRESPONDING EFFECTIVE MIGRATION VELOCITY

Inlet Gas Velocity (m/s)	Applied Voltage (kV)	Total Discharge Current due to Corona Suppression, I_0 (mA)	Total Mass Collection Efficiency (-80 kV, I_0)	EMV (cm/s)
1.2	80	3.0	97.6%	6.22
1.6	79.8	2.4	95.0%	6.66
2.0	79.2	2.25	92.7%	7.27
2.7	78.2	1.95	87.1%	7.68
3.7	76.6	1.5	77.0%	7.55
5.5	73.3	0.75	61.7%	7.33

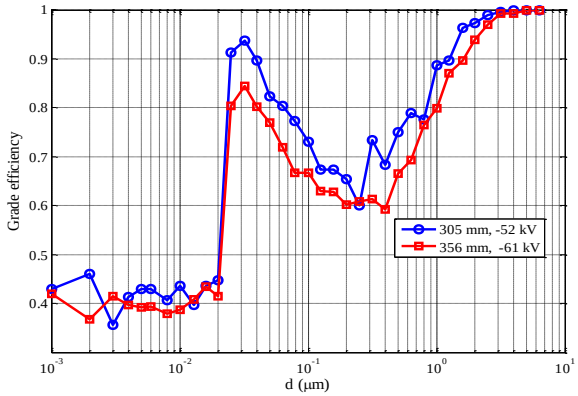

Fig. 8. Fractional Collection Efficiency versus Particle Diameter 305mm and 356mm Tubes with Saw Tooth Disks; Inlet Gas Velocity is 2.7 m/s.

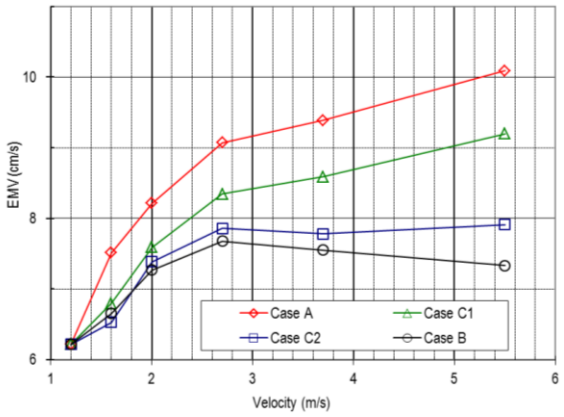

Fig. 9. Effective Migration Velocity Versus Inlet Gas Velocity

velocity for case A and B is shown in Fig. 9. It is clear that for constant power (Case A), the EMV increases with velocity, whereas for varying input power (Case B), the EMV first rises to a peak and then reduces only gradually. This is surprising in that the power is reduced substantially, up to over 75%. Two intermediate additional cases were calculated in which the voltage was held constant and two different levels of current reduction were assumed (Case C1 and C2 in Fig. 9).

Since the actual operating points at different particle loadings were based on some assumptions, it is possible that for a higher inlet velocity, the applied voltage to the discharge electrode drops even more than assumed in the current simulations. It is believed that both the effects of corona discharge quenching and lower excitation voltage will result in lower total mass collection efficiency for higher inlet gas velocity; it is just a matter of degree. As there is no re-entrainment as in a dry ESP, it is expected that the influence of increased velocity on performance would not be as severe in a WESP.

IV. CONCLUSIONS

Computational models of WESPs were developed. The effect of gas flow rate, voltage distance and particulate loading on precipitation performance was investigated for a given particle size distribution and electrical operating characteristics. Total mass and fractional collection efficiency and the corresponding theoretical and EMV were calculated. The variation of EMV versus tube velocity was investigated for assumed variation in secondary voltage and current. It was shown that the model is a useful tool in explaining the limits to which velocity can be raised without major degradation in performance.

ACKNOWLEDGMENT

The authors gratefully acknowledge the financial support by MITACS of Canada. This work was made possible by the facilities of the SHARCNET Canada.

REFERENCES

[1] H.J. White, *Industrial electrostatic precipitation, Addison-Wesley*, Pergamon Press, 1963, pp. 74-125.

[2] P. Saiyasitpanich, T. C. Keener, S.-J. Khang and M. Lu, "Removal of diesel particulate matter (DPM) in a tubular wet electrostatic precipitator", *J. Electrostat*., vol. 65, pp. 618-624, 2007.

[3] N. Farnoosh, "Three-dimensional modeling of electrostatic precipitator using hybrid finite element - flux corrected transport technique," Ph.D. dissertation, Dept. Elect. Comput. Eng., Univ. of Western Ontario, 2011.

[4] D. Brocilo, J. Podlinski, J.S. Chang, J. Mizeraczyk and R.D. Findlay, "Electrode geometry effects on the collection efficiency of submicron and ultra fine dust particles in spike-plate electrostatic precipitators", *J. Phys.: Conf. Ser.*, vol. 142, no. 1, pp. 1-6, 2008.

[5] L. M. Dumitran, P. Atten and D. Blanchard, "Numerical simulation of fine particles charging and collection in an electrostatic precipitator with regular barbed electrodes", *Inst. Phys. Conf. Ser*., no. 178, pp. 199-205, 2003.

[6] P. A. Lawless, "Particle charging bounds, symmetry relations and an analytic charging rate model for the continuum regime", *J. Aerosol Sci*., vol. 27, no. 2, pp. 191-215, 1996.

[7] N. Farnoosh, K. Adamiak and G.S.P. Castle," 3D numerical analysis of EHD turbulent flow and mono-disperse charged particle transport and collection in a wire-plate ESP," *J. Electrostat*., vol. 68, no. 6, pp. 513-522, 2010.

[8] N. Farnoosh, K.Adamiak and G.S.P. Castle," Numerical calculations of submicron particle removal in a spike-plate electrostatic precipitator," *IEEE Trans. Dielectr. Electr. Insul*, vol. 18, no. 5, pp. 1439-1452, 2011.

[9] N. Farnoosh, "Computational modeling of WESPs," *UWO-TurboSonic Inc Internal Correspondence*, 2011.

[10] C. Riehle, "Mass flux and effective migration velocity in electrostatic precipitators", *Powder Technol*., vol. 86, no. 1, pp. 95-102, 1996.

[11] C.A. Easton, J. Lethbridge and R.A. Allan, "Controlling power boiler emissions with wet electrostatic precipitators - Elk Falls wet precipitator installation," *TAPPI International Environmental Conference & Exhibit*, Montreal, Quebec, 2002.